Journal of Molecular Catalysis A: Chemical 337 (2011) 61–67

Contents lists available at ScienceDirect

Journal of Molecular Catalysis A: Chemical

journal homepage: www.elsevier.com/locate/molcata

Preparation, characterization and activity evaluation of V_2O_5–$LaVO_4$ composites under visible light irradiation

Yiming He[a,*], Yongjiao Wang[b], Leihong Zhao[b], Xintao Wu[c], Ying Wu[b,*]

[a] Department of Materials Physics, Zhejiang Normal University, Jinhua 321004, China
[b] Institute of Physical Chemistry, Zhejiang Key Laboratory for Reactive Chemistry on Solid Surfaces, Zhejiang Normal University, Jinhua 321004, China
[c] State Key Laboratory of Structural Chemistry, Fujian Institute of Research on the Structure of Matter, Chinese Academy of Sciences, Fuzhou, 350002, China

ARTICLE INFO

Article history:
Received 9 November 2010
Received in revised form
21 December 2010
Accepted 7 January 2011
Available online 21 January 2011

Keywords:
Photocatalytic oxidation
$LaVO_x$ composite
Visible light
Acetone

ABSTRACT

This article presents a novel visible-light-driven catalyst, an $LaVO_x$ composite that was prepared from $La(NO_3)_3$ and NH_4VO_3 solutions. The visible-light-induced photocatalytic activity of this composite was evaluated by the degradation of acetone. Results indicate that the $LaVO_x$ composite exhibits high activity for acetone photodegradation. The highest acetone conversion (93.1%) was obtained with the $La_1V_{1.5}O_x$ catalyst. Its photo-activity and ability for complete oxidation could be enhanced further by doping with a small amount of the metal platinum. Physical and photophysical properties of the $LaVO_x$ composite catalysts were evaluated by X-ray diffraction (XRD), the Brunauer–Emmett–Teller (BET) method, Raman spectroscopy (Raman), Fourier transform infrared spectroscopy (FT-IR), scanning electron microscopy (SEM), UV–vis diffuse reflectance spectroscopy (DRS), and photoluminescence (PL) spectroscopy. Based on the results of this investigation, the coupling effect of m-$LaVO_4$ and V_2O_5 was identified as generating the high activity in catalysis.

1. Introduction

Photocatalysis, utilizing solar energy and semiconductors, is of great importance in solving the energy crisis and environmental issues [1,2]. In the past two decades, significant efforts have been devoted to developing novel oxide semiconductor photocatalysts that can be applied in environmental purification and water-splitting, to generate hydrogen by conversion of light energy [1–4]. However, no satisfactory photocatalyst has been found as yet. Therefore, research toward new photocatalytic materials are of important.

In recent times, orthovanadates have garnered scientific attention due to their V 3d orbital electron, which can be activated by visible light. This property makes them potential candidates as photocatalytic material, and a range of vanadates (e.g., $InVO_4$, $BiVO_4$, $CeVO_4$, $SmVO_4$, $M_2V_2O_8$ [M = Mg, Ni, Zn], Ag_3VO_4, etc.) has been studied for their photocatalytic activity [5–10]. However, some disadvantages, such as small specific surface areas, long migration distances for excited electron–hole pairs, and increasing energy-wasteful recombination have been noted, all of which are expected to detract from the photocatalytic ability. In order to obtain satisfactory activity, the orthovanadate photocatalysts are usually modified by three methods: loading of noble metal, doping with metal ions and coupling with metal oxide [11–20]. The work function of noble metal is usually higher than that of vanadate and, therefore, electrons can be removed from vanadate particles in the vicinity of each metal particle. This results in the formation of Schottky barriers at each metal–semiconductor interface and leads to charge separation. Thus, the loading noble metal (e.g., Pt, Pd, Ag) can promote photocatalytic activity [11–13]. However, the added noble metal would add to the cost of the photocatalyst and limits its practical application at a larger scale. Doping metal ions into the vanadate photocatalyst is another method to improve the photocatalytic activity [14–17]. Bellakki et al. synthesized the Pd-ion-doped $CeVO_4$ using the solution combustion method [15]. The substitution of Pd ions was found to enhance photocatalytic activity. Madras et al. reported that the doping of Li, Ca, and Fe, instead of Pd, into $CeVO_4$ can also improve photocatalytic efficiency [16]. However, the enhanced activity is usually limited due to the low mobility of the carriers in the doping levels. In addition, the doped photocatalyst always incurs problems due to the discrete doping levels. Compared with the above two methods, coupling a metal oxide can actually be considered as the most promising method to improve the activity of vanadate in terms of its high efficiency in the separation of electron–hole pairs and associated low costs. Several research studies that focused on the metal-oxide-coupled vanadate composite have been reported [18–22]. Long et al. [18] reported

* Corresponding authors. Tel.: +86 0579 82283920; fax: +86 0579 82283920.
E-mail addresses: hym@zjnu.cn (Y. He), ying-wu@zjnu.cn (Y. Wu).

1381-1169/$ – see front matter © 2011 Elsevier B.V. All rights reserved.
doi:10.1016/j.molcata.2011.01.015

that the coupling of Co_3O_4 into $BiVO_4$ can highly promote the photocatalytic efficiency in the phenol-degradation reaction. This enhanced activity was attributed to the coupling effect of Co_3O_4 and $BiVO_4$ in retarding the recombination of electron–hole pairs. Similar results were also observed for the NiO/$InVO_4$ couple catalyst [19]. In addition to NiO and Co_3O_4, V_2O_5 was found to be a good co-catalyst to promote the separation of electron–hole pairs [20–22].

$LaVO_4$ has garnered considerable interest in recent times because of its surface catalytic properties, optical properties, and especially the absorption of visible light [23–25]. Its photocatalytic activity in benzene degradation has also been studied by Fu et al. [26]. However, results reported from Fu's research indicate that $LaVO_4$ presents poor photocatalytic activity due to its fast recombination of electron–hole pairs. This result is also substantiated by Zhou's work [27]. Therefore, it seems that pure $LaVO_4$ is not a good photocatalyst, and it requires modification to improve its photocatalytic activity. In this article, we report the preparation of a novel composite material comprising $LaVO_4$ and V_2O_5 by a simple, soft chemical method. This $LaVO_x$ composite exhibits strong photocatalytic activity for the decomposition of acetone as well as high photocatalytic stability in gas-phase reactions under visible light irradiation.

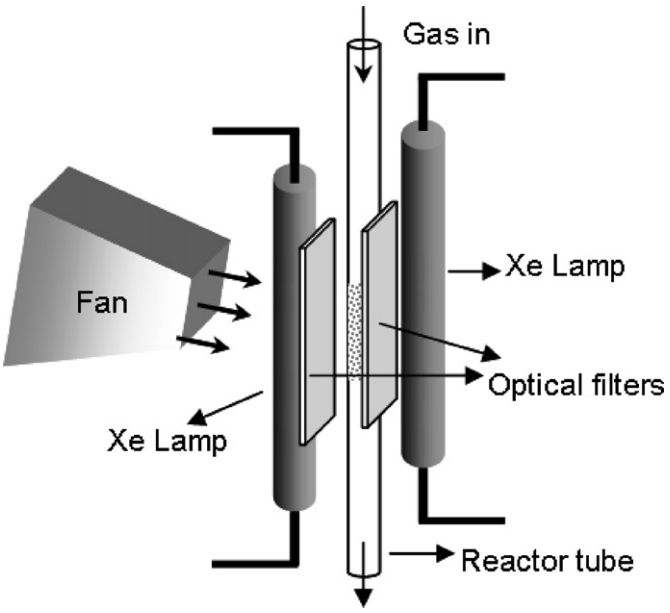

Fig. 1. The reactor system.

2. Experimental

2.1. Catalyst preparation

NH_4VO_3 (>99%), La_2O_3 (>99.99%), EDTA (>99%), and P25 (Degussa TiO_2) as the reference, were purchased commercially and used without further purification. The V_2O_5 was obtained by calcining ammonium metavanadate at 500 °C for 4 h. The $LaVO_x$ composite catalysts were prepared as detailed in the following: solutions of NH_4VO_3 and $La(NO_3)_3$ (obtained by dissolving La_2O_3 in HNO_3), with different V/La molar ratio, were mixed and evaporated to obtain a solid precursor. The solid was dried at 100 °C for 12 h, then calcined at 500 °C for 4 h, and then cooled to room temperature to yield the catalyst.

t-$LaVO_4$ (tetragonal phase) was prepared by the hydrothermal method [28]: 0.004 mol of $La(NO_3)_3$ aqueous solution, 0.004 mol of NH_4VO_3 solution, and 0.0004 mol of EDTA solution were mixed with vigorous stirring. The pH value of the mixture was adjusted to 6 by the addition of NH_3 solution. The final volume of the mixture was kept as 80 mL. After stirring for 10 min, the mixture was transferred into a Teflon-lined stainless steel autoclave with a capacity of 100 mL for hydrothermal treatment at 180 °C for 24 h. As the autoclave cooled to room temperature naturally, the precipitation was separated by centrifugation, washed with distilled water and absolute ethanol, and dried under vacuum at 100 °C.

m-$LaVO_4$ (monoclinic phase) was prepared by the precipitation method: solutions of NH_4VO_3 and $La(NO_3)_3$ with a V/La molar ratio of 1.0, were mixed to obtain a precipitate. The pH value of the solution was adjusted to 5 with an NH_3 solution. The precipitate deposited was filtered, washed three times by water, dried at 100 °C for 12 h and calcined at 600 °C for 4 h.

The 0.1 wt.% Pt/$La_1V_{1.5}O_x$ catalyst was prepared by the impregnation–photoreduction method [9]: 4.5 g of $La_1V_{1.5}O_x$ catalyst was added to 3.0 mL of $H_2PtCl_6{\cdot}6H_2O$ solution (Pt: 0.0015 g/mL). The sample was kept in the dark for 5 h, and then dried at 80 °C for 10 h. Thereafter, the dried sample was irradiated by a Xe lamp for 2 h to obtain the 0.1 wt.% Pt/$La_1V_{1.5}O_x$ catalyst.

The mixture of V_2O_5 and m-$LaVO_4$ with a V/La molar ratio of 1.5, was prepared by a mechanical method by grinding in an agate mortar without any calcination.

2.2. Activity testing

The catalytic reaction under visible light was carried out in a quartz tube (ID 5.0 mm) reactor. Two 400 W xenon lamps were used as visible light sources, and in front of the Xe lamps, there were optical filters ($\lambda > 380$ nm) to eliminate UV light. In either reactor, the volume of catalyst (about 100 mg for P25 and 600–900 mg for other samples) was about 1.0 mL. A thermocouple was placed in the center of the catalyst bed to detect the reaction temperature. The reactor tube was cooled by a powerful fan. Because of the heat from the lamps, although we tried to cool down the reactor by the fan, the reaction temperature was still between 120 and 130 °C. Pure oxygen was used as the oxidant. The organic reactants (acetone, methanol, 2-propanal, and benzene) were fed into the reactor by bubbling gas (O_2) through liquid organic at 0 °C (cooled in a water-ice bath) to obtain the reactant mixture. The flow of the mixture was controlled at 6.0 mL/min. The concentrations of acetone (10 mol%), methanol (5 mol%), 2-propanal (1 mol%), and benzene (2.2 mol%) were analyzed by GC. Before each catalytic testing, the photocatalyst was allowed to equilibrate in the reaction gas for at least 60 min. The reaction products were analyzed on a gas chromatograph (GC-7890||, equipped with a GDX-203 column and a 5A carbon molecular sieve column) with a thermal conductor detector. The catalyst activity and selectivity as well as the mol concentration of organics were calculated by the area normalized method. All the data were collected after 3 h of online reaction.

In order to rule out the thermal reaction, both the $La_1V_{1.5}O_x$ and 0.1 wt.% Pt/$La_1V_{1.5}O_x$ catalysts were tested for acetone oxidation in the dark at the same reaction temperature (130 °C). The dark reaction shows that acetone did not react with oxygen over $La_1V_{1.5}O_x$ or 0.1 wt.% Pt/$La_1V_{1.5}O_x$ catalysts at 130 °C. The blank reaction was also tested. The result shows that no acetone was photodegradated without photocatalyst under visible light ($\lambda > 380$ nm) (Fig. 1).

2.3. Catalysts characterization

The XRD characterization of catalysts was carried out on an X-ray diffraction spectroscopy meter (RIGAKU DMAX2500) using Cu Kα radiation (40 kV/40 mA). The specific surface areas of the catalysts were measured on Autosorb-1 (Quantachrome Instruments). The FTIR spectra of the catalysts were recorded on PerkinElmer

Table 1
Specific surface area of catalysts.

Catalysts	S (m^2/g)	Catalysts	S (m^2/g)
La_2O_3	9	$La_1V_{1.5}O_x$	21
m-$LaVO_4$	11	$La_1V_{2.5}O_x$	19
t-$LaVO_4$	43	$La_1V_{3.5}O_x$	24
$La_1V_1O_x$	30	$La_1V_{4.5}O_x$	17
$La_1V_{1.2}O_x$	39	V_2O_5	6

Magna 750 with a resolution of 4 cm^{-1}. The visible-light Raman spectra of catalysts were collected on RM1000 spectrometer (Renishaw) with an Ar ion laser (514.5 nm) as the excitation source. Scanning electron microscope (SEM) was carried out on Hitachi S-4800 at 10 kV. The corresponding energy dispersive X-ray (EDX) analysis was operated at an accelerating voltage of 20 kV. The absorption spectra of the catalysts, or UV–vis diffuse reflectance spectra, were obtained in the range of 200–800 nm at room temperature using a UV–vis spectrophotometer (PerkinElmer Lambda900) equipped with an integrating sphere attachment. $BaSO_4$ was used as the reflectance standard. The photoluminescence (PL) spectra of catalysts were collected on FLS-920 (Edinbergh Instrument). The light source was a Xe lamp (excitation at 254 nm).

3. Results and discussion

3.1. BET, XRD, and FT-IR characterizations

Nitrogen-sorption experiments indicate that both La_2O_3 and V_2O_5 have low specific surface areas (<10 m^2/g). In comparison with La_2O_3 or V_2O_5, the t-$LaVO_4$ has a much larger specific surface area (43 m^2/g). However, m-$LaVO_4$ (11 m^2/g) exhibits a low surface area. The BET surface area of these $LaVO_x$ composites is in the range of 17–39 m^2/g (Table 1) and the highest value was observed for the $La_1V_{1.2}O_x$ composite (39 m^2/g). However, no direct association between the BET surface area and V/La molar ratio has been observed.

The crystal composition and phase structure of the samples were examined by XRD. Fig. 2 depicts the XRD patterns of these catalysts. Pure La_2O_3 is in the hexagonal phase, and shows several strong diffraction peaks at 2θ = 15.5°, 25.9°, 29.0°, 29.8°, and 39.4° (JCPDS05-0602). Pure $LaVO_4$ has two crystal phases (monoclinic and tetragonal phases) and exhibits different peaks in the XRD pattern. In general, m-$LaVO_4$ constitutes the thermodynamically stable state, while t-$LaVO_4$ is metastable and cannot be generated by conventional methods [29]. The $LaVO_x$ composites were prepared using a simple solution method. Therefore, m-$LaVO_4$ was considered the main phase and observed in the XRD pattern of $LaVO_x$ composites. In an evaluation of the $La_1V_1O_x$ catalyst, t-$LaVO_4$ was detected in addition to m-$LaVO_4$, however, the diffraction peak was not strong. With increasing V concentration, the peak intensity of the t-$LaVO_4$ phase decreased. When the V/La ratio was 1.5, t-$LaVO_4$ disappeared and only m-$LaVO_4$ was observed. Further, for the samples with V/La ratio higher than 1.0, several signals at 15.2°, 21.7°, and 34.2°, which can normally be assigned to the V_2O_5 phase, were observed, and its peak intensity was found to be directly proportional to the V/La molar ratio. With the exception of the V_2O_5 and $LaVO_4$ phases, no new phase was found in the $LaVO_x$ composites.

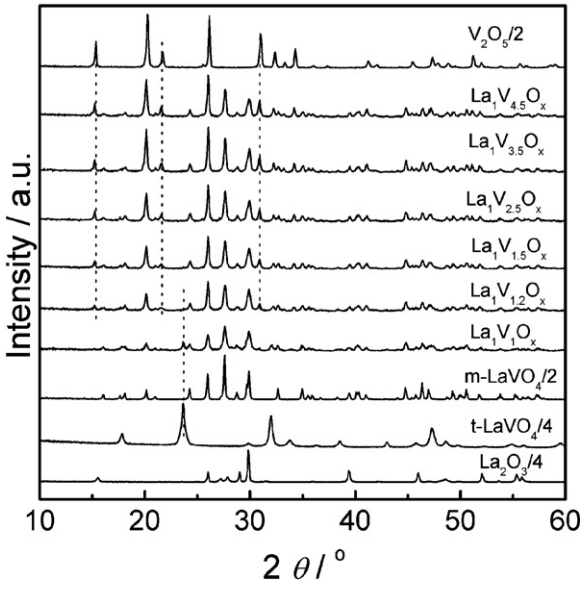

Fig. 2. XRD patterns of catalysts.

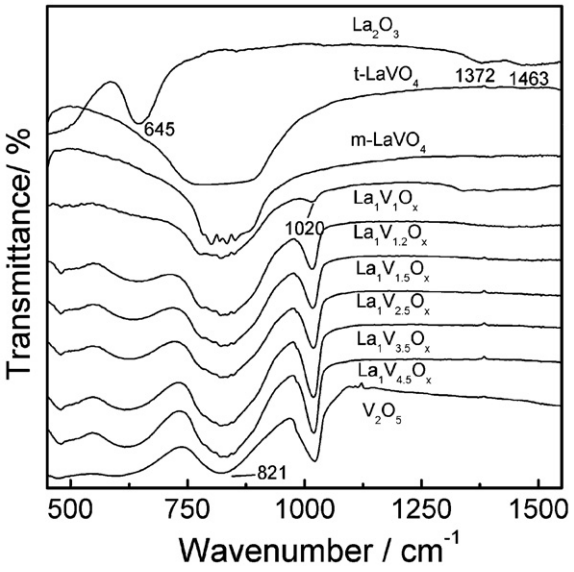

Fig. 3. FT-IR spectra $LaVO_x$ composites.

Fig. 3 depicts the FT-IR spectra of the $LaVO_x$ composite catalysts. La_2O_3 presents one strong peak at 645 cm^{-1} and two weak peaks at 1372 and 1463 cm^{-1} [30]. m-$LaVO_4$ presents several peaks at 783, 802, 821, 836, and 852 cm^{-1}, while t-$LaVO_4$ only generates a broad band in the 730–980-cm^{-1} region [31,32]. For the $La_1V_1O_x$ catalyst, both the m-$LaVO_4$ and La_2O_3 phase are detected. Further, another peak at 1020 cm^{-1} was observed in the spectrum of $La_1V_1O_x$. From the published literature, this peak could be assigned to the V=O stretching vibration in the V_2O_5 phase [33]. Therefore, it is apparent that some La and V have not reacted and exist in this oxide phase over the $La_1V_1O_x$ catalyst. However, when the V/La ratio was higher than 1.0, the La_2O_3 phase disappeared and only $LaVO_4$ and V_2O_5 were observed in the $LaVO_x$ composites. With increasing V concentration, the peak intensity of V_2O_5 also increased, and this is consistent with the XRD result.

3.2. Raman and SEM characterizations

Both the XRD and FT-IR characterizations could only provide information on the phase structure, but do not present any information with regard to the surface structure. To correct this information lacuna, the study samples were characterized in a Raman experiment. Fig. 4 depicts the Raman spectra of $LaVO_x$ composites and the reference oxides. Similar to reports in the literature [34,35], the Raman bands that are centered at 282, 303, 403, 480, 526, 699, and

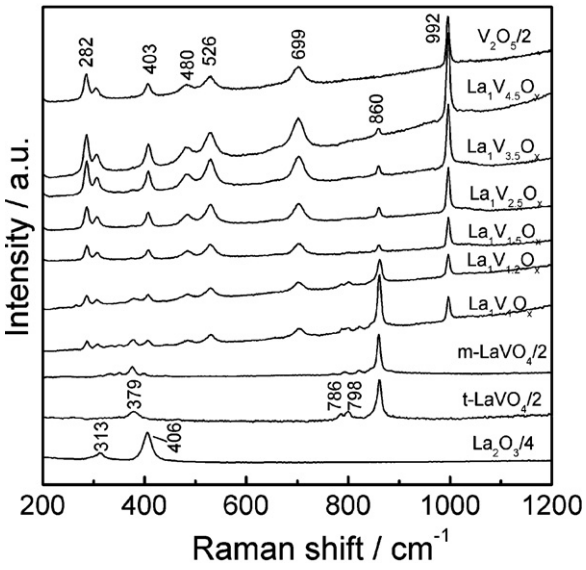

Fig. 4. Raman spectra of $LaVO_x$ composites.

992 cm^{-1} are assigned to V_2O_5, whereas the peaks at 313 cm^{-1} and 406 cm^{-1} are assigned to La_2O_3 [36]. t-$LaVO_4$ shows two strong Raman bands at 379 cm^{-1} and 860 cm^{-1} that correspond with the vibrations of the La–O and VO_4 groups, respectively [26]. m-$LaVO_4$ exhibits almost the same spectrum with the exception of several weak bands at 332, 351, and 399 cm^{-1} [26]. The decreased number of vibration peaks observed for t-$LaVO_4$ is in accordance with the lower coordination number (8) and the high symmetry (*D2d*) of the La^{3+} ions—both of which contribute to the relatively simple vibration spectra as compared with that of m-$LaVO_4$ [26]. As shown in Fig. 4, all these $LaVO_x$ composites have peaks that can be assigned to V_2O_5 or $LaVO_4$. At relatively lower vanadium concentrations, the Raman bands of $LaVO_4$ are stronger than that of V_2O_5. However, when the V/La molar ratio is higher than 1.2, the bands generated by V_2O_5 are much stronger than those of $LaVO_4$. Nonetheless, it is impossible to determine the phase type of $LaVO_4$ due to its weak Raman bands. However, the Raman result clearly demonstrates that there are V_2O_5 and $LaVO_4$ domains on the surface of these $LaVO_x$ catalysts. Combined with the data in Figs. 2 and 3, it can be concluded that the $LaVO_4$ and V_2O_5 phases are well distributed in the photocatalyst. This result can also be proved by the SEM experiment. As shown in Fig. 5, the molar ratio of La to V at different time points is similar and close to the theoretical value. The EDX result also indicates that some of the vanadium is concentrated on the surface of catalyst, which might be due to the method employed to prepare the catalyst. The enrichment of V on the catalyst surface also explains the weak bands of $LaVO_4$ in the Raman spectra of these $LaVO_x$ catalysts.

3.3. UV–vis characterizations

The optical absorption property of a semiconductor, which is relevant to the electronic structure, is recognized as the key factor determining its photocatalytic activity. Fig. 6a shows the UV–vis diffuse reflectance spectra of t-$LaVO_4$, m-$LaVO_4$, and V_2O_5. t-$LaVO_4$ only manifests a capacity to absorb the UV light and shows the color white. The band-gap-absorption edge is determined to be 352 nm, which corresponds with the band-gap energy of 3.52 eV, and is consistent with the results reported by Manivanan [37]. As opposed to t-$LaVO_4$, m-$LaVO_4$ and V_2O_5 can absorb most of the visible light and manifest orange yellow and brick-red colors, respectively. Their band-gap energy is determined to be 2.20 eV (m-$LaVO_4$) and 2.13 eV(V_2O_5). The UV–vis spectra of the P25 (TiO_2 Degussa), La_2O_3 and $LaVO_x$ catalysts are shown in Fig. 6b. Similar to t-$LaVO_4$, both La_2O_3 and P25 can only absorb UV light ($\lambda < 400$ nm). On the contrary, the $LaVO_x$ composite exhibits a better photoabsorbtion performance, which might be attributed to the contributions by m-$LaVO_4$ and V_2O_5. As the V_2O_5 presents a higher ability for photoabsorbtion, the V concentration shows a great effect on the light-absorption performance. As shown in Fig. 6b, with increasing V/La ratio, the photoabsorption performance of the $LaVO_x$ compos-

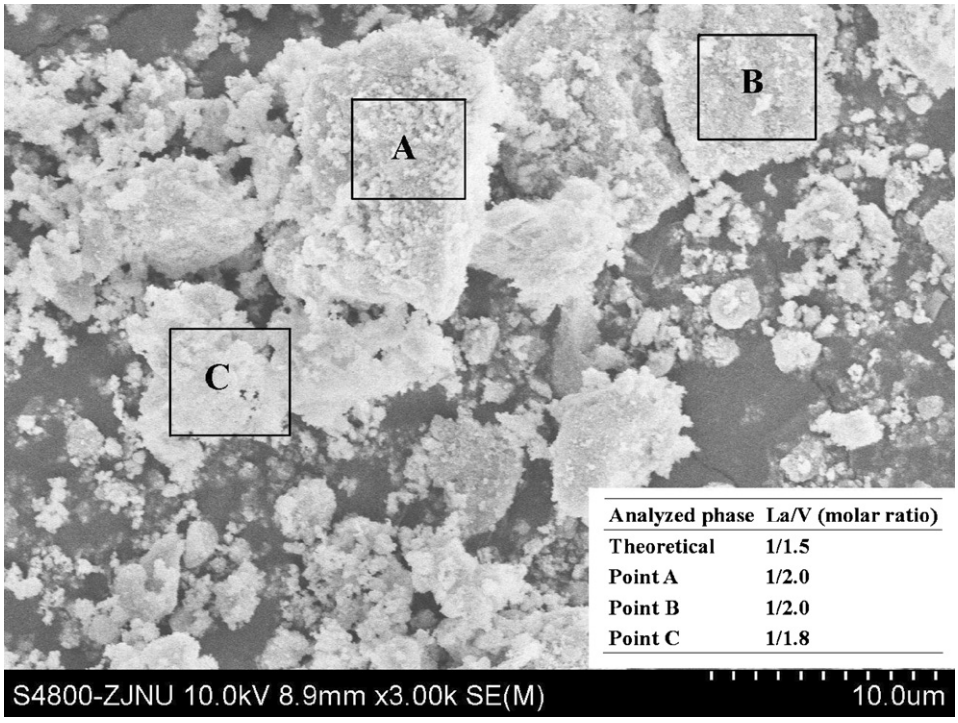

Fig. 5. SEM photograph of a representative catalyst $La_1V_{1.5}O_x$.

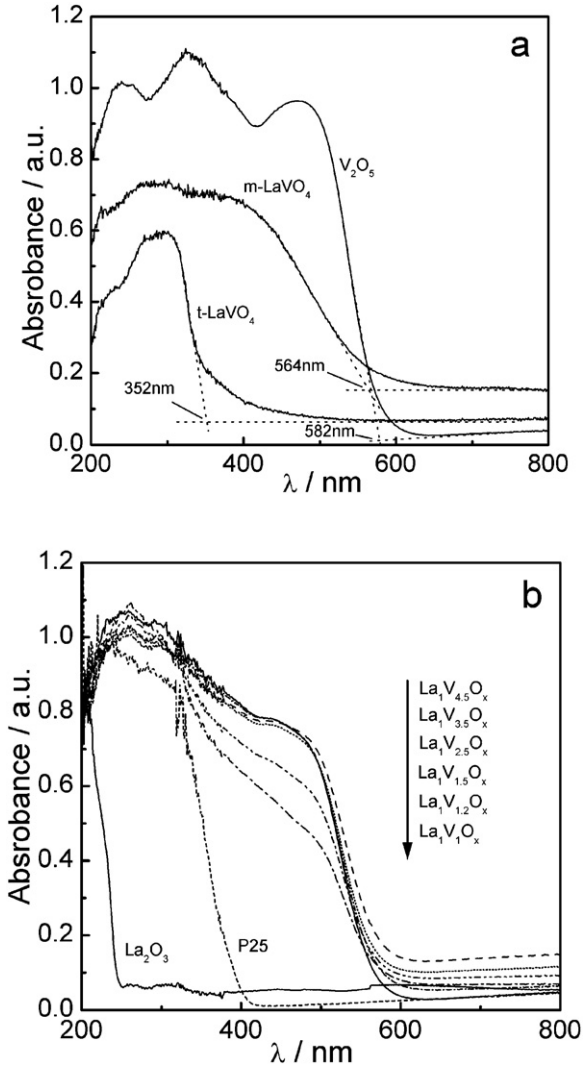

Fig. 6. UV–vis diffuse absorption spectra of $LaVO_4$, V_2O_5 (a) and $LaVO_x$ composites (b).

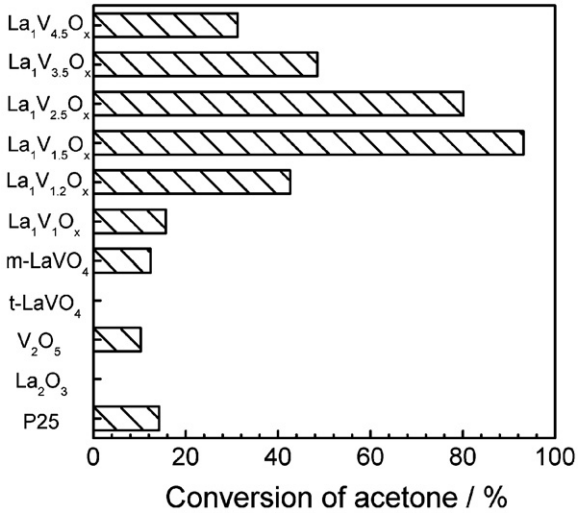

Fig. 7. Photocatalytic activity of catalysts under visible light irradiation (λ > 380 nm).

ites improves. However, when the V/La ratio is larger than 1.5, only a slight difference is observed.

3.4. Photocatalytic activity

Acetone degradation was used as the probe reaction to evaluate the activity of the catalyst. Fig. 7 presents the photocatalytic activities of P25 (TiO_2 Degussa), La_2O_3, V_2O_5 and the $LaVO_x$ composite when subjected to visible light irradiation (λ > 380 nm). No acetone was photodegradated with La_2O_3 and t-$LaVO_4$ as catalysts, which could be due to their bad photoabsorption performance with visible light. For the same reason, P25 exhibits low activity under visible light, although it is well known that P25 is a good catalyst under UV light irradiation. V_2O_5 also exhibited low acetone conversion similar to P25 and this is attributed to the rapid recombination of electron–hole pairs [11]. For the $LaVO_x$ composite catalysts, it is found that the concentration of V greatly influences their catalytic performance. With the increase of V to the La molar ratio, the acetone conversion initially increased and, then, decreased. At a V/La molar ratio of 1.5, the catalyst exhibited the highest activity for acetone degradation, and 93.1% conversion of acetone was achieved. However, it should be noted that the typical degradation products are CO_2, CO, acetol, and H_2O during the photodegradation of acetone. For example, only about 55.3% of acetone was completely degraded to CO_2 and H_2O with $La_1V_{1.5}O_x$ as the catalyst ($STY_{CO_2} = 60.8$ mg/g_{Cat}/h). A significant amount of CO and acetol were released as partial oxidation products, and these are also considered pollutants. In order to overcome this defect, we doped the $La_1V_{1.5}O_x$ composite with a small amount of Pt. It has been reported in the published literature that the doping of Pt is a practical method for achieving complete oxidation of organic pollutants [11]. Table 2 presents the test results for the Pt-doped $La_1V_{1.5}O_x$ catalyst under visible light. Higher photocatalytic activity (99.5% conversion of acetone) was obtained over 0.1 wt.% Pt/$La_1V_{1.5}O_x$ catalyst and almost all the acetone was converted to CO_2 and H_2O ($STY_{CO_2} = 117$ mg/g_{Cat}/h). Further, it was proven to be efficient in the oxidation of methanol, 2-propanol, and benzene (Table 2). Therefore, it is apparent that the $LaVO_x$ composite exhibits high performance in photodegradation reactions and holds promise for practical application in technology that undertakes air purification.

3.5. Discussion

In general, the specific surface area of a catalyst is considered to be an important factor influencing the activity of the catalysts. A high surface area in a catalyst is desirable for good adsorption of reactant, which could promote the catalytic reaction. However, the high surface area can also generate surface defects, which are considered to constitute recombination centers for electron–hole pairs. Therefore, in the field of photocatalysis, the specific surface area is usually not consistent with the photocatalytic activity [38,39]. In the present study, the $La_1V_{1.5}O_x$ catalyst exhibited the highest activity, but its BET surface area (21 m^2/g) was smaller than that of the $La_1V_1O_x$ (39 m^2/g) and $La_1V_{2.5}O_x$ (19 m^2/g) catalysts. This indicates that the specific surface area does not play a major role in influencing catalytic activity. The most important factor impacting on catalytic activity might be the composition of the catalysts themselves.

The XRD and FT-IR experiments revealed that $LaVO_x$ composites were composed of m-$LaVO_4$, t-$LaVO_4$, La_2O_3, and V_2O_5 phases. Combined with the results in Fig. 7, we note that the catalyst comprising m-$LaVO_4$ and V_2O_5 exhibited higher activity than the catalyst containing the La_2O_3 or t-$LaVO_4$ phase. This indicates that La_2O_3 is not beneficial in retarding the combination of electron–hole pairs, and m-$LaVO_4$ and V_2O_5 may be the active phases. However, as shown in Fig. 7, the V_2O_5 phase manifests low activity. Further, the performance of m-$LaVO_4$ is also not suitably high (12.4% conversion of acetone). Zhou et al. [27] have

Table 2
Photocatalytic performance of $La_1V_{1.5}O_x$ and 0.1 wt.% $Pt/La_1V_{1.5}O_x$ catalysts under visible light irradiation ($\lambda > 380$ nm).

Organics	Catalysts	Conv./mol%	Selectivity/mol%			STY_{CO_2} ($mg/g_{Cat}/h$)
			CO_2	CO	Others	
Acetone	$La_1V_{1.5}O_x$	93.1	55.3	43.5	1.2[a]	60.8
	0.1 wt.% $Pt/La_1V_{1.5}O_x$	99.5	99.6	0.0	0.4[a]	117
Methanol	$La_1V_{1.5}O_x$	98.5	23.1	76.9	0.0	13.4
	0.1 wt. %$Pt/La_1V_{1.5}O_x$	100	100	0.0	0.0	58.9
2-Propanol	$La_1V_{1.5}O_x$	92.5	63.0	33.0	4.0[b]	7.1
	0.1 wt.% $Pt/La_1V_{1.5}O_x$	100	99.2	0.0	0.8[b]	11.7
Benzene	$La_1V_{1.5}O_x$	40.2	67.9	13.9	8.2[c]	9.0
	0.1 wt.% $Pt/La_1V_{1.5}O_x$	87.3	93.2	0.0	6.8[c]	21.1

Notes: STY_{CO_2} represents space time yield of CO_2.
[a] Represents acetol.
[b] Represents acetone.
[c] Represents unknown byproduct.

reported that m-$LaVO_4$ is inactive in the photodegradation of acetone. Therefore, it appears likely that the high activity of the $LaVO_x$ catalyst does not originate from the single phase of m-$LaVO_4$ or V_2O_5. The coupling effect between m-$LaVO_4$ and V_2O_5 might constitute a more suitable explanation. Several researchers have noted the specificity of the photoactivity of composite systems that have two semiconductors in contact with each other [9–11,18–22], and have attributed the improved activity to the enhanced charge separation, which is due to the electron or hole transfer between the coupled semiconductors. In the present study, we concur that this mechanism appears to act in these catalysts.

Fig. 8 depicts the schematic electronic band structure of the $LaVO_4$–V_2O_5 composite and the charge-transfer process under visible light irradiation. The band potential of V_2O_5 was obtained from the work published by Liu [40]. The flat band potential of $LaVO_4$ can be calculated by the equation:

$$V_{fb}(\mathrm{SHE}) = 2.94 - E_g,$$

where V_{fb} is the flat band potential and E_g is the band gap. The relationship between the flat band potential and band gap was suggested by Scaife [41], and can be used to predict the band-edge positions theoretically for the oxide that does not contain partly filled d-levels (e.g., $InVO_4$, $NiNb_2O_6$, $NiTa_2O_6$, and $LaVO_4$) [41–44]. The conduction band of t-$LaVO_4$ is more negative than the conduction band of m-$LaVO_4$ and V_2O_5 (Fig. 8). The electron transfer from V_2O_5 or m-$LaVO_4$ is impossible. Therefore, the t-$LaVO_4$ would demonstrate no contribution to the separation of electron–hole pairs. On the contrary, the valence and conduction bands of m-$LaVO_4$ and V_2O_5 are disposed suitably, and electron or hole transfers can occur from one semiconductor to another. This simultaneous charge transfer could increase the space charge separation, limit electron–hole recombination and, thus, promote photo-oxidation efficiency.

This hypothesis was proved by the PL experiment, which elucidates the migration, transfer, and recombination processes of the photogenerated electron–hole pairs in a semiconductor. As shown in Fig. 9, the PL spectrum of m-$LaVO_4$ shows a strong emission between 430 and 550 nm, which indicates that the electrons and holes recombine rapidly [45,46]. However, over $La_1V_{1.5}O_x$ catalyst, the peak intensity is greatly decreased. This suggests that the doping with V_2O_5 decreases the electron–hole pair recombination.

The physical mixture of V_2O_5 and m-$LaVO_4$, which has the same V/La ratio as the $La_1V_{1.5}O_x$ composite, was also prepared and tested in the photodegradation of acetone under visible light irradiation. Test results indicate the mixture demonstrates an acetone conversion of 37.5%, which is much higher than that of the pure phase (V_2O_5 and m-$LaVO_4$). This result provides further proof for our hypothesis. However, when compared with the $La_1V_{1.5}O_x$ composite, the photo-activity of the mixture is very low. It might be attributed to the bad contact between V_2O_5 and $LaVO_4$, which would retard the charge transfer between the two semiconductors and decrease the separation efficiency of the electron–hole

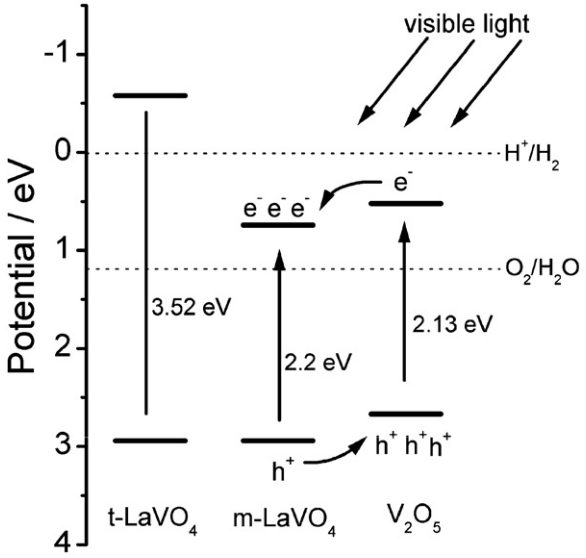

Fig. 8. Schematic electronic band structure of $LaVO_4$–V_2O_5 composite and the charge-transfer process under visible light irradiation.

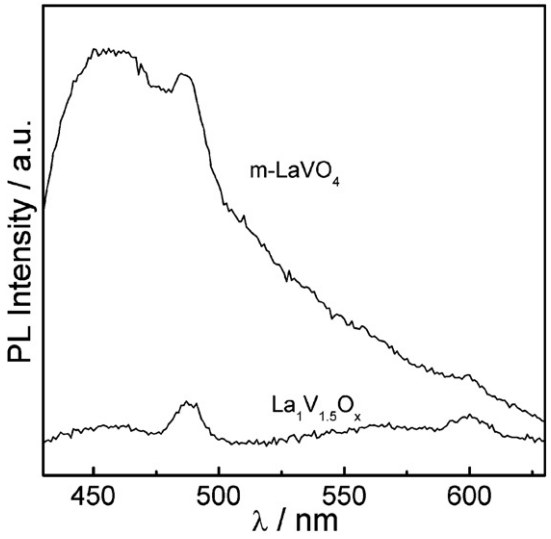

Fig. 9. PL spectra of m-$LaVO_4$ and $La_1V_{1.5}O_x$ composite.

pairs [47]. Therefore, the physical mixing does not appear be a good method for synthesizing the coupled photocatalyst. However, it might be interesting to carefully study the effective coupling of two different semiconductors.

4. Conclusions

In summary, a series of $LaVO_x$ composites with different V/La molar ratios were synthesized using the solution method and then tested in the acetone photodegradation reaction. Results indicate that the $LaVO_x$ composite exhibits high photocatalytic activity under visible light. The optimal V/La molar ratio was found to be 1.5. Higher vanadium concentration was found to reduce the activity of the catalyst. By doping a small amount of Pt, the catalytic performance of $La_1V_{1.5}O_x$ catalyst could be promoted further. The characterization indicates that $LaVO_x$ composites were mainly composed of m-$LaVO_4$ and V_2O_5 phases. Their valence and conduction bands are disposed suitably, and, therefore, electron or hole transfer can occur between m-$LaVO_4$ and V_2O_5. By this mechanism, the recombination of electron–hole pairs is retarded and the mechanism is considered as the source of the high activity of $LaVO_x$ composites.

Acknowledgements

This work was supported by the National Natural Science Foundation of China (21003109) and the Doctor Startup Fund of Zhejiang Normal University (ZC304008169).

References

[1] A.L. Linsebigler, G. Lu Jr., J.T. Yates, Chem. Rev. 95 (1995) 735–758.
[2] A. Kudo, H. Kato, I. Tsuji, Chem. Lett. 33 (2004) 1534–1539.
[3] A. Fujishima, T.N. Rao, D.A. Tryk, J. Photochem. Photobiol. C: Photochem. Rev. 1 (2000) 1–21.
[4] K. Rajeshwar, N.R.D. Tacconi, C.R. Chenthamarakshan, Chem. Mater. 13 (2001) 2765–2782.
[5] J.H. Ye, Z.G. Zou, M. Oshikiri, A. Matsushita, M. Shimoda, M. Imai, T. Shishido, Chem. Phys. Lett. 356 (2002) 221–226.
[6] A. Kudo, K. Ueda, H. Kato, I. Mikami, Catal. Lett. 53 (1998) 229–230.
[7] A.P. Zhang, J.Z. Zhang, N.Y. Cui, X.Y. Tie, Y.W. An, L.J. Li, J. Mol. Catal. A: Chem. 304 (2009) 28–32.
[8] S. Mahapatra, R.G. Madras, T.N. Guru Row, Ind. Eng. Chem. Res. 46 (2007) 1013–1017.
[9] Y.M. He, T.L. Sheng, J.S. Chen, R.B. Fu, S.M. Hu, X.T. Wu, Catal. Commun. 10 (2009) 1354–1357.
[10] S.F. Chen, W. Zhao, W. Liu, H.Y. Zhang, X.L. Yu, Y.H. Chen, J. Hazard. Mater. 172 (2009) 1415–1423.
[11] F. Chen, J. Wang, J.Q. Xu, X.P. Zhou, Appl. Catal. A: Gen. 348 (2008) 54–59.
[12] Z.L. Jin, X.J. Zhang, G.X. Lu, S.B. Li, J. Mol. Catal. A: Chem. 259 (2006) 275–280.
[13] L.Q. Jing, D.J. Wang, B.Q. Wang, S.D. Li, B.F. Xin, H.G. Fu, J.Z. Sun, J. Mol. Catal. A: Chem. 244 (2006) 193–200.
[14] M.R. Dolgos, A.M. Paraskos, M.W. Stoltzfus, S.C. Yarnell, P.M. Woodward, J. Solid State Chem. 182 (2009) 1964–1971.
[15] M.B. Bellakki, T. Baidya, C. Shivakumara, N.Y. Vasanthacharya, M.S. Hegde, G. Madras, Appl. Catal. B: Environ. 84 (2008) 474–481.
[16] S. Mahapatra, R. Vinu, D. Saha, T.N. Guru Rowa, G. Madras, Appl. Catal. A: Gen. 361 (2009) 32–41.
[17] S. Mahapatra, G. Madras, T.N. Guru Row, J. Phys. Chem. C 111 (2007) 6505–6511.
[18] M. Long, W. Cai, J. Cai, B. Zhou, X. Chai, Y. Wu, J. Phys. Chem. B 110 (2006) 20211–20216.
[19] H.Y. Lin, Y.F. Chen, Y.W. Chen, Int. J. Hydrogen Energy 32 (2007) 86–92.
[20] M.A. Rauf, S.B. Bukallah, A. Hamadi, A. Sulaiman, F. Hammadi, Chem. Eng. J. 129 (2007) 167–172.
[21] C.W. Zou, Y.F. Rao, A. Alyamani, W. Chu, M.J. Chen, D.A. Patterson, E.A.C. Emanuelsson, W. Gao, Langmuir 26 (2010) 11615–11620.
[22] M. Shahid, I. Shakir, S.J. Yang, D.J. Kang, Mater. Chem. Phys. 124 (2010) 619–622.
[23] Z.M. Fang, Q. Hong, Z.H. Zhou, S.J. Dai, W.Z. Weng, H.L. Wan, Catal. Lett. 61 (1999) 39–44.
[24] K. Li, C. Huang, Ind. Eng. Chem. Res. 45 (2006) 7096–7100.
[25] J.W. Stouwdam, M. Raudsepp, F.V. Veggel, Langmuir 21 (2005) 7003–7008.
[26] H.J. Huang, D.Z. Li, Q. Li, W.J. Zhang, Y. Shao, Y.B. Chen, M. Sun, X.Z. Fu, Environ. Sci. Technol. 43 (2009) 4164–4168.
[27] J. Wang, F. Chen, X.P. Zhou, J. Phys. Chem. C 112 (2007) 9723–9729.
[28] C.J. Jia, L.D. Sun, L.P. You, X.C. Jiang, F. Luo, Y.C. Pang, C.H. Yan, J. Phys. Chem. B 109 (2005) 3284–3290.
[29] W.L. Fan, X.Y. Song, S.X. Sun, X. Zhao, J. Solid State Chem. 180 (2007) 284–290.
[30] S.J. Huang, A.B. Walters, M.A. Vannice, Appl. Catal. B: Environ. 26 (2000) 101–108.
[31] T. Tojo, Q. Zhang, F. Saito, J. Alloys Compd. 427 (2007) 219–222.
[32] J. Ma, Q.S. Wu, Y.P. Ding, J. Nanopart. Res. 10 (2008) 775–786.
[33] T. Ono, Y. Tanaka, T. Takeuchi, K. Yamamoto, J. Mol. Catal. A: Chem. 159 (2000) 293–300.
[34] G.C. Bond, S.F. Tahir, Appl. Catal. 71 (1991) 1–31.
[35] X.J. Wang, H.D. Li, Y.J. Fei, X. Wang, Y.Y. Xiong, Y.X. Nie, K.A. Feng, Appl. Surf. Sci. 177 (2001) 8–14.
[36] E. Rodríguez-Reyna, A.F. Fuentes, M. Maczka, J. Hanuza, K. Boulahya, U. Amador, J. Solid. State Chem. 179 (2006) 522–531.
[37] P. Parhi, V. Manivanan, Solid State Sci. 10 (2008) 1012–1019.
[38] A. Rachel, M. Subrahmanyam, P. Boule, Appl. Catal. B: Environ. 37 (2002) 301–308.
[39] A. Rachel, M. Sakakha, M. Subrahmanyam, P. Boule, Appl. Catal. B: Environ. 37 (2002) 293–300.
[40] Z.B. Wu, D. Fan, Y. Liu, H.Q. Wang, Catal. Commun. 11 (2009) 82–85.
[41] D.E. Scaife, Solar Energy 25 (1980) 41–54.
[42] J.H. Ye, Z.G. Zou, H. Arakawa, M. Oshikiri, M. Shimoda, A. Matsushita, T. Shishido, J. Photochem. Photobiol. A: Chem. 148 (2002) 79–83.
[43] J.H. Ye, Z.G. Zou, A. Matsushita, Int. J. Hydrogen Energy 28 (2003) 651–655.
[44] Q.Z. Wang, H. Liu, J. Yuan, W.F. Shangguan, Chin. J. Catal. 30 (2009) 565–569.
[45] J.Y. Shi, J. Chen, Z.C. Feng, T. Chen, Y.X. Lian, X.L. Wang, C. Li, J. Phys. Chem. C 111 (2007) 693–699.
[46] J.W. Tang, Z.G. Zou, J.H. Ye, J. Phys. Chem. B 107 (2003) 14265–14269.
[47] X.P. Lin, F.Q. Huang, J.C. Xing, W.D. Wang, F.F. Xu, Acta Mater. 56 (2008) 2699–2705.